

Inelastic neutron scattering study of magnetic interactions in $\text{CsMn}_x\text{Mg}_{1-x}\text{Br}_3$. I. Spin waves in CsMnBr_3

U. Falk and A. Furrer

*Labor für Neutronenstreuung, Eidgenössische Technische Hochschule Zürich,
CH-5303 Würenlingen, Switzerland*

H. U. Güdel

Institut für Anorganische Chemie, Universität Bern, CH-3000 Bern, Switzerland

J. K. Kjems

Risø National Laboratory, DK-4000 Roskilde, Denmark

(Received 6 October 1986)

The inelastic neutron scattering technique was used to determine the dispersion of the spin-wave excitations of the triangular antiferromagnet CsMnBr_3 below $T_N = 8.3$ K. Two spin-wave branches of transverse and longitudinal symmetry were observed which are excellently described on the basis of a spin-wave model including an intrachain exchange coupling $J = -890 \pm 10$ μeV , an interchain exchange coupling $J'' = -1.7 \pm 0.1$ μeV , and a single-ion anisotropy parameter $D = 12 \pm 1$ μeV . The small value of the ratio J''/J indicates the one-dimensional magnetic character of CsMnBr_3 . Care has to be taken in the interpretation of the observed energy spectra with respect to two-magnon scattering contributions. Our data are consistent with the recently observed spin-wave energy gap of CsMnBr_3 in the one-dimensional state.

I. INTRODUCTION

A major breakthrough in the understanding of magnetism occurred sixty years ago with the discovery of quantum mechanical exchange by Heisenberg¹ and Dirac.² Later their ideas were generalized by Van Vleck.³ The Heisenberg-Dirac-Van Vleck (HDVV) model assumes pairwise magnetic interactions of the form

$$\mathcal{H} = -2 \sum_{i>j} J_{ij} \mathbf{S}_i \cdot \mathbf{S}_j, \quad (1)$$

where J_{ij} is an effective exchange parameter and \mathbf{S}_i is the spin operator of the i th ion. The HDVV model is an extremely powerful model for the interpretation of a wide variety of magnetic properties of S -state systems. Obviously it is of fundamental interest to know both the signs and magnitudes of the exchange parameters as well as the limitations of the applicability of the HDVV model. Quantum-mechanical calculations of exchange interactions, both on an *ab-initio* level and with a variety of approximations, can claim only qualitative accuracy. The most reliable information thus results from experimental data. Measurements of the magnetic properties and the heat capacity have long been used to derive exchange parameter values. Spin-wave dispersions, obtained by inelastic neutron scattering (INS), provide a valuable source of information about exchange parameters. The potential of ferro- and antiferromagnetic resonance, NMR, and optical spectroscopy (magnon sidebands) has more recently been realized. There are principal difficulties, however, in the derivation of exchange parameters from experimental data in magnetically ordered materials. Except for a few

low-dimensional situations it is not possible to obtain exact theoretical solutions of the relevant effective Hamiltonian. The sum of pairwise interactions has to be restricted, and certain approximations have to be made in the underlying statistical concept. In addition, effects such as higher-order exchange coupling may not manifest themselves directly in the physical properties under examination. Nevertheless, there is an alternative method which bypasses the difficulties that arise with cooperative systems. This alternative method is to study a few magnetic ions which are exchange coupled among themselves and isolated in a "nonmagnetic" matrix. The advantage of studying such magnetic clusters is that the model can be treated exactly, as only a small number of interactions are present and cooperative effects do not occur. Hence, an unambiguous comparison of theory and experiment is possible as outlined in paper II.

In the present paper we present INS experiments on CsMnBr_3 . The crystal structure is hexagonal, space group $P6_3/mmc$, and consists of chains of Mn^{2+} ions along the c axis with an intrachain separation of 3.26 Å, whereas the interchain distance amounts to 7.91 Å.⁴ Because of the simple, spin-only ground state of the Mn^{2+} ions ($S = \frac{5}{2}$) the exchange interaction is expected to be of the HDVV-type. Neutron diffraction, magnetic susceptibility, and specific-heat measurements showed that three-dimensional magnetic ordering occurs at $T_N = 8.3$ K.⁵ Below T_N the Mn^{2+} moments are coupled antiferromagnetically along the chains but lie in the basal plane, where they form a triangular array. The magnitude of the Mn^{2+} moment extrapolated to 0 K amounts to about 3.3 μ_B .⁵ This low value can be explained by the existence

of a substantial zero-point spin deviation, which reflects the basically one-dimensional nature of the magnetic coupling.⁶ Indeed, above T_N neutron scattering maxima were observed at reciprocal lattice planes,⁷ indicative of one-dimensional correlations along the chains which subsist up to about 50 K.

Various attempts to determine the exchange interaction from the magnetic thermodynamic properties provided values for the nearest-neighbor intrachain coupling between -970 and $-850 \mu\text{eV}$.^{5,7} There is no doubt, however, that a more reliable value results from an analysis of the spin-wave dispersion. From INS experiments carried out in the ordered phase a nearest-neighbor intrachain interaction $J = -880 \pm 10 \mu\text{eV}$ and a nearest-neighbor interchain interaction $J'' = -1.9 \pm 0.3 \mu\text{eV}$ were obtained,⁸ i.e., the exchange along the c axis is almost 3 orders of magnitude larger than in other directions, which confirms the one-dimensional magnetic behavior of CsMnBr_3 . The spin waves measured in the one-dimensional magnetic state have similar energies to those found below T_N , but no dispersion is observed for wave vectors perpendicular to the c axis as expected.^{9,10}

The INS measurements of the spin-wave dispersion in CsMnBr_3 reported so far⁸⁻¹⁰ are not sufficiently detailed to allow an unambiguous interpretation, since only one spin-wave branch was observed. Although the spin-wave branches are nearly degenerate along the $\langle 001 \rangle$ direction, an appreciable splitting may be expected for the spin waves perpendicular to the c axis, particularly in the vicinity of the magnetic Brillouin zone centers. Therefore we decided to reinvestigate the spin-wave spectrum of CsMnBr_3 with the aim to resolve the low-energy spin excitations and to study in detail the energy gap at zero wave vector, which provides direct information about the

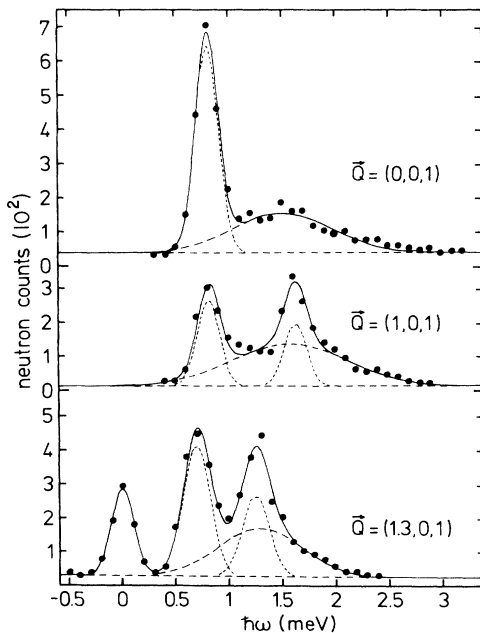


FIG. 1. Energy spectra of neutrons scattered from CsMnBr_3 . The temperature was 6 K for the upper spectrum and 4.2 K for the lower two spectra.

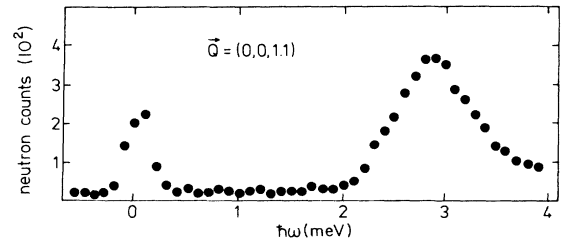


FIG. 2. Energy spectrum of neutrons scattered from CsMnBr_3 at $T = 6$ K.

magnetic anisotropy. As we will show below, our data clarify the recent controversy concerning the analysis of the spin-wave energy gap observed for CsMnBr_3 in the one-dimensional state.^{9,10}

II. EXPERIMENTAL RESULTS

The INS experiments were performed at the DR3 reactor in Risø and at the reactor Saphir in Würenlingen. The high-resolution scans were performed at Risø with the use of the triple-axis spectrometer TAS7 which is installed at a neutron guide connected to a cold H_2 source. The scattered-neutron energy was held constant at 5 meV giving rise to an energy resolution of 0.28 meV. At Würenlingen we used the triple-axis spectrometer R2 with the scattered-neutron energy kept fixed at 13.7 meV giving rise to an energy resolution of about 1 meV. The single crystal of CsMnBr_3 was prepared as described in detail in paper II. A cylinder of 0.7 cm diameter and 1.2 cm length was oriented so as to place the (101) plane into the scattering plane. The measurements were carried out in the neutron energy-loss configuration for scattering vectors $\mathbf{Q} = (Q_x, 0, Q_z)$, i.e., for spin waves propagating along the $\langle 100 \rangle$ and $\langle 001 \rangle$ directions. The majority of the data were taken below T_N .

Typical high-resolution energy spectra are shown in Figs. 1 and 2. Clearly two spin-wave excitations are observed along the $\langle 100 \rangle$ direction. The peak positions of the spin-wave excitations versus wave vector $\mathbf{q} = (\xi_x, \xi_y, \xi_z)$ are shown in Fig. 3. The background of the energy spectra displayed in Fig. 1 exhibits a broad cusp centered between 1 and 1.5 meV which is due to two-magnon scattering. The spectral distribution of the two-magnon scattering contributions is considerably tem-

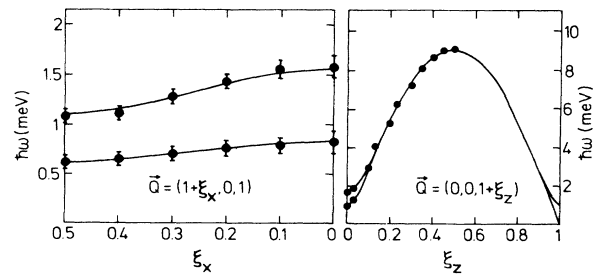


FIG. 3. Observed and calculated spin-wave dispersions of CsMnBr_3 at $T = 6$ K.

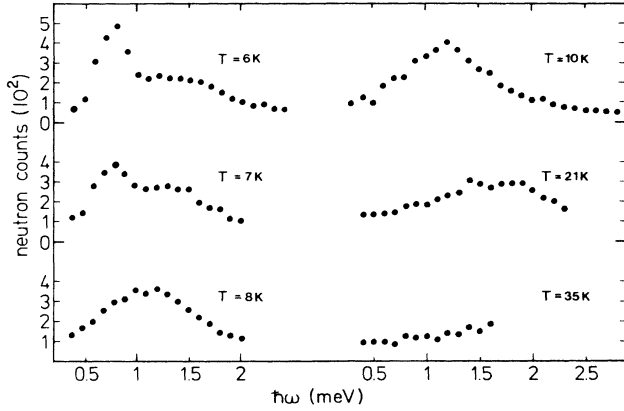


FIG. 4. Temperature dependence of one- and two-magnon scattering contributions to the energy spectra of neutrons scattered from CsMnBr₃ for $\mathbf{Q}=(0,0,1)$.

perature dependent as shown in Fig. 4. Upon raising the temperature the mean energy is shifted upwards and the intensity increases, reaching a maximum at about 10 K, and then decreases and disappears above 40 K. On the other hand, the one-magnon scattering is dominant at low temperatures as expected; its intensity decreases with increasing temperature and disappears in the two-magnon background for $T > 10$ K.

III. THEORY

Following Eq. (1) and restricting the exchange to nearest-neighbor intra- and interchain interactions J and J'' , respectively, the relevant spin Hamiltonian for CsMnBr₃ reads

$$\mathcal{H} = -2J \sum_{i>j} \mathbf{S}_i \cdot \mathbf{S}_j - 2J'' \sum_{i>j} \mathbf{S}_i \cdot \mathbf{S}_j + D \sum_i (S_i^z)^2. \quad (2)$$

The anisotropy term with $D > 0$ forces the spins into the xy plane. On the basis of Eq. (2) we obtain the following expression for the spin-wave dispersion of a triangular antiferromagnet with ordering wave vector $\mathbf{k}_0 = (\frac{1}{3}, \frac{1}{3}, 1)$:^{11,12}

$$\hbar\omega(\mathbf{q}) = 2S\sqrt{u(\mathbf{q})v(\mathbf{q})}, \quad (3)$$

with

$$u(\mathbf{q}) = 4|J| \sin^2 \left[\frac{\pi\xi_z}{2} \right] + |J''| [3 - f(\xi_x, \xi_y)],$$

$$v(\mathbf{q}) = 4|J| \cos^2 \left[\frac{\pi\xi_z}{2} \right] + |J''| [3 + 2f(\xi_x, \xi_y)] + D, \quad (4)$$

$$f(\xi_x, \xi_y) = \cos(2\pi\xi_x) + \cos(2\pi\xi_y) + \cos[2\pi(\xi_x + \xi_y)].$$

The neutron cross section has the following form:¹³

$$\frac{d^2\sigma}{d\Omega d\omega} \sim F^2(\mathbf{Q}) \sum_{\alpha,\beta} \left[\delta_{\alpha\beta} - \frac{Q_\alpha Q_\beta}{Q^2} \right] \sum_{i,j} e^{i\mathbf{Q}\cdot(\mathbf{R}_i - \mathbf{R}_j)} \sum_{\lambda} p_{\lambda} \int dt e^{-i\omega t} \langle \lambda | S_i^\alpha(0) S_j^\beta(t) | \lambda \rangle, \quad (5)$$

where $F(\mathbf{Q})$ denotes the form factor and p_{λ} the population of the state $|\lambda\rangle$. Terms with $\alpha \neq \beta$ vanish. For $\alpha = \beta = z$ we have

$$\left[\frac{d^2\sigma}{d\Omega d\omega} \right]^{zz} \sim F^2(\mathbf{Q}) \left[1 - \left[\frac{Q_z}{Q} \right]^2 \right] \sum_{\mathbf{q}} \left[\frac{u(\mathbf{q})}{v(\mathbf{q})} \right]^{1/2} [n(\omega_{\mathbf{q}}) + \frac{1}{2} \mp \frac{1}{2}] \delta(\omega \pm \omega_{\mathbf{q}}) \delta(\mathbf{Q} - \boldsymbol{\tau} \pm \mathbf{q}). \quad (6)$$

where $n(\omega_{\mathbf{q}})$ is the Bose occupation number. The upper and lower signs denote processes in which a single spin wave of energy $\omega_{\mathbf{q}}$ is annihilated and created, respectively. For $\alpha = \beta = x$ and $\alpha = \beta = y$ expansion of the operators S_i^x and S_i^y in powers of $1/S$ yields in first order

$$\left[\frac{d^2\sigma}{d\Omega d\omega} \right]^{xx,yy} \sim F^2(\mathbf{Q}) \left[1 + \left[\frac{Q_z}{Q} \right]^2 \right] [n(\omega_{\mathbf{q}}) + \frac{1}{2} \mp \frac{1}{2}] \delta(\omega \pm \omega_{\mathbf{q}})$$

$$\times \left[\sum_{\mathbf{q}} \left[\frac{v(\mathbf{q} + \mathbf{k}_0)}{u(\mathbf{q} + \mathbf{k}_0)} \right]^{1/2} \delta(\mathbf{Q} - \boldsymbol{\tau} + \mathbf{k}_0 \pm \mathbf{q}) + \sum_{\mathbf{q}} \left[\frac{v(\mathbf{q} - \mathbf{k}_0)}{u(\mathbf{q} - \mathbf{k}_0)} \right]^{1/2} \delta(\mathbf{Q} - \boldsymbol{\tau} - \mathbf{k}_0 \pm \mathbf{q}) \right]. \quad (7)$$

Equations (6) and (7) suggest that for a given scattering vector \mathbf{Q} realized, e.g., in the neutron energy-loss configuration three spin waves with different energies are created, namely $\hbar\omega(\mathbf{Q} - \boldsymbol{\tau})$, $\hbar\omega(\mathbf{Q} - \boldsymbol{\tau} + \mathbf{k}_0)$, and $\hbar\omega(\mathbf{Q} - \boldsymbol{\tau} - \mathbf{k}_0)$, which can readily be identified according to the polarization factors in the cross-section formula. For CsMnBr₃ we have $D, |J''| \ll |J|$, thus strong spin-wave intensities are expected for scattering vectors \mathbf{Q} with the z component Q_z close to any odd integer.

Expanding the spin operators of Eq. (5) up to second order yields the neutron cross-section for two-magnon scattering:

$$\begin{aligned}
\left[\frac{d^2\sigma}{d\Omega d\omega} \right]^{2 \text{ magnons}} &\sim F^2(\mathbf{Q}) \left[1 + \left[\frac{Q_z}{Q} \right]^2 \right] \times \sum_{\mathbf{q}} \sum_{\mathbf{k}=\pm\mathbf{k}_0} \left[\frac{1}{4} \sinh(2\theta_{\mathbf{q}}) \sinh(2\theta_{\mathbf{Q}+\mathbf{k}-\mathbf{q}}) + \sinh^2\theta_{\mathbf{q}} \sinh^2\theta_{\mathbf{Q}+\mathbf{k}-\mathbf{q}} \right] \\
&\quad \times n(\omega_{\mathbf{q}}) [n(\omega_{\mathbf{Q}+\mathbf{k}-\mathbf{q}}) + 1] \delta(\omega + \omega_{\mathbf{q}} - \omega_{\mathbf{Q}+\mathbf{k}-\mathbf{q}}) \\
&\quad + \left[\frac{1}{4} \sinh(2\theta_{\mathbf{q}}) \sinh(2\theta_{\mathbf{Q}+\mathbf{k}-\mathbf{q}}) + \sinh^2\theta_{\mathbf{q}} \cosh^2\theta_{\mathbf{Q}+\mathbf{k}-\mathbf{q}} \right] n(\omega_{\mathbf{q}}) n(\omega_{\mathbf{Q}+\mathbf{k}-\mathbf{q}}) \delta(\omega + \omega_{\mathbf{q}} + \omega_{\mathbf{Q}+\mathbf{k}-\mathbf{q}}) \\
&\quad + \left[\frac{1}{4} \sinh(2\theta_{\mathbf{q}}) \sinh(2\theta_{\mathbf{Q}+\mathbf{k}-\mathbf{q}}) + \cosh^2\theta_{\mathbf{q}} \sinh^2\theta_{\mathbf{Q}+\mathbf{k}-\mathbf{q}} \right] [n(\omega_{\mathbf{q}}) + 1] [n(\omega_{\mathbf{Q}+\mathbf{k}-\mathbf{q}}) + 1] \delta(\omega - \omega_{\mathbf{q}} - \omega_{\mathbf{Q}+\mathbf{k}-\mathbf{q}}) \\
&\quad + \left[\frac{1}{4} \sinh(2\theta_{\mathbf{q}}) \sinh(2\theta_{\mathbf{Q}+\mathbf{k}-\mathbf{q}}) + \cosh^2\theta_{\mathbf{q}} \cosh^2\theta_{\mathbf{Q}+\mathbf{k}-\mathbf{q}} \right] [n(\omega_{\mathbf{q}}) + 1] n(\omega_{\mathbf{Q}+\mathbf{k}-\mathbf{q}}) \delta(\omega - \omega_{\mathbf{q}} + \omega_{\mathbf{Q}+\mathbf{k}-\mathbf{q}}),
\end{aligned} \tag{8}$$

with

$$\tanh(2\theta_{\mathbf{q}}) = \frac{4 |J| \cos(\pi \xi_z) - 3 |J''| f(\xi_x, \xi_y) + D}{4 |J| + |J''| [6 - f(\xi_x, \xi_y)]}. \tag{9}$$

Since there is no fixed correlation between the scattering vector \mathbf{Q} and the magnon wave vectors, two-magnon scattering does not give rise to well-defined excitations, but broad distributions are expected in the energy spectra.

IV. ANALYSIS OF RESULTS

For the scattering vectors $\mathbf{Q}=(Q_x, 0, Q_z)$ realized in the present experiments the spin-wave energies $\hbar\omega(\mathbf{Q}-\boldsymbol{\tau}+\mathbf{k}_0)$ and $\hbar\omega(\mathbf{Q}-\boldsymbol{\tau}-\mathbf{k}_0)$ are degenerate, thus we expect to observe two spin-wave branches with energies $\hbar\omega(\mathbf{Q}-\boldsymbol{\tau})$ and $\hbar\omega(\mathbf{Q}-\boldsymbol{\tau}\pm\mathbf{k}_0)$ corresponding to longitudinal (zz) and transverse (xx, yy) excitations, respectively, as shown in Figs. 1 and 2. For $\mathbf{Q}=(0, 0, Q_z)$ the longitudinal mode disappears due to the polarization factor of Eq. (6), and the transverse excitations are roughly degenerate except for Q_z close to any integer. The energy spectra were analyzed in terms of Gaussian fits to the observed spin-wave peaks, whose widths are essentially determined by the instrumental resolution as given by the elastic line for spin waves propagating along the $\langle 100 \rangle$ direction, whereas the widths of the spin-wave peaks propagating along the $\langle 001 \rangle$ direction were considerably broadened due to the steep slope of the dispersion. The two-magnon contributions were also approximated by a Gaussian, although the corresponding cross section, Eq. (8), may yield a more complicated form. The experimental spin-wave energies at $T=6$ K (Fig. 3) were interpreted on the basis of Eq. (3) which provided the following least-squares fitted model parameters:

$$\begin{aligned}
J &= -890 \pm 10 \text{ } \mu\text{eV}, \\
J'' &= -1.7 \pm 0.1 \text{ } \mu\text{eV}, \\
D &= 12 \pm 1 \text{ } \mu\text{eV}.
\end{aligned}$$

The calculated spin-wave dispersion is in excellent agreement with the experimental data as shown in Fig. 3.

Although the two-magnon scattering contributions can be calculated from Eq. (8), its application to interpret the present data is made difficult for the following reason. Most experiments were performed for scattering vectors

$\mathbf{Q}=(Q_x, 0, 1)$, thus we have from Eq. (9) $\tanh(2\theta_{\mathbf{q}}) \approx 1$, since $|J''|, D \ll 1$. This means that the argument $2\theta_{\mathbf{q}}$ is not well defined due to the statistical uncertainties of the model parameters, and consequently the cross section (8) cannot be reliably determined. Nevertheless Eq. (8) qualitatively predicts the observed features of the two-magnon scattering contributions. The main contributions to the two-magnon scattering come from magnon pairs with wave vectors lying both in reciprocal planes with integer values of ξ_z and corresponding magnon energies in the range $0 \leq \hbar\omega \leq 1.5$ meV. Therefore the two-magnon scattering is expected to cover the energy range $0 \leq \hbar\omega \leq 3$ meV, in agreement with our observations. For scattering vectors with noninteger values of Q_z the two-magnon scattering drastically decreases; it is already absent for $\mathbf{Q}=(0, 0, 1.1)$ as illustrated in Fig. 2.

V. DISCUSSION

The exchange parameters of CsMnBr_3 determined in the present work essentially agree with the results of earlier INS experiments,⁸ and the anisotropy parameter compares well with $D = \pm 12 \text{ } \mu\text{eV}$ derived from EPR measurements of CsMgBr_3 doped with Mn^{2+} ions.¹⁴ From our experiments we clearly obtain $D > 0$, so that the Mn^{2+} moments are forced to lie perpendicular to the c axis in agreement with the neutron diffraction results.⁵

Our model parameters may be used to calculate various physical properties of CsMnBr_3 . For the Néel temperature Hennessy *et al.*¹⁵ derived the following relationship:

$$T_N = \frac{4}{3k_B} S(S+1) \frac{1}{0.64} (JJ'')^{1/2}. \tag{10}$$

Inserting the exchange parameters obtained in the present work yields $T_N = 8.2$ K, which is in excellent agreement with the observed Néel temperature of 8.3 K. The observed magnetic susceptibility⁵ is well reproduced by our model parameters in the high temperature region, whereas considerable discrepancies arise for $T < 100$ K. The agreement can be markedly improved by the inclusion of biquadratic exchange interactions,¹⁶ which will be discussed in detail in paper II.

Finally our model parameters may be used to interpret the spin-wave energy gap of 1.7 ± 0.2 meV observed for CsMnBr_3 in the one-dimensional state.^{9,10} The spin-wave dispersion of a one-dimensional magnet is given by¹⁷

$$\hbar\omega(\xi_z) = 4 |J| S \left[\left\{ 1 + \left| \frac{D}{8J} \right| \right\}^2 - \{\cos(2\pi\xi_z)\}^2 \right]^{1/2}. \quad (11)$$

From our model parameters we obtain a spin-wave energy gap ($\xi_z=0$) of 0.52 meV. Another source of anisotropy lies in the dipolar forces between the spins which has been calculated for the one-dimensional Heisenberg antiferromagnet.¹⁸ This calculation has no disposable parameters and predicts an energy gap of 1.2 meV for CsMnBr₃. The sum of the single-ion and dipolar anisotropy gap thus amounts to 1.7 meV as experimentally observed.^{9,10}

In conclusion, we have shown that the spin-wave dispersions of CsMnBr₃ are well reproduced by the

effective Hamiltonian (2), in which the exchange coupling is restricted to bilinear nearest-neighbor interactions within and between the chains. The quality of the data did not warrant an inclusion of more distant neighbor interactions. Higher-order interactions can principally not be determined from spin-wave dispersion data.¹⁹ In paper II we will demonstrate that next-nearest neighbor as well as biquadratic two- and three-spin interactions contribute to the effective intrachain parameter J in Eq. (2).

ACKNOWLEDGMENT

Financial support by the Swiss National Science Foundation is gratefully acknowledged.

¹W. Heisenberg, *Z. Phys.* **38**, 411 (1926).

²P. A. M. Dirac, *Proc. R. Soc. London, Ser. A* **112**, 661 (1926).

³J. H. Van Vleck, *The Theory of Electric and Magnetic Susceptibilities* (University Press, Oxford, 1932).

⁴J. Goodyear and D. J. Kennedy, *Acta Cryst. B* **28**, 1640 (1972).

⁵M. Eibschütz, R. C. Sherwood, F. S. L. Hsu, and D. E. Cox, in *Magnetism and Magnetic Materials—Proceedings of the Conference on Magnetism and Magnetic Materials, 1972, Denver*, AIP Conf. Proc. No. 10, edited by C. D. Graham and J. J. Rhyne (AIP, New York, 1972), p. 684.

⁶P. A. Montano, E. Cohen, and H. Shechter, *Phys. Rev. B* **6**, 1053 (1972).

⁷W. J. Fitzgerald, D. Visser, and K. R. A. Ziebeck, *J. Phys. C* **15**, 795 (1982).

⁸W. Breitling, W. Lehmann, R. Weber, N. Lehner, and V. Wagner, *J. Magn. Magn. Mater.* **6**, 113 (1977).

⁹M. F. Collins and B. D. Gaulin, *J. Appl. Phys.* **55**, 1869 (1984).

¹⁰B. D. Gaulin and M. F. Collins, *Can. J. Phys.* **62**, 1132 (1984).

¹¹See, e.g., H. Kadowaki, K. Hirakawa, and K. Ubukoshi, *J. Phys. Soc. Jpn.* **52**, 1799 (1983).

¹²R. Feile, J. K. Kjems, A. Hauser, H. U. Güdel, U. Falk, and A. Furrer, *Solid State Commun.* **50**, 435 (1984).

¹³See, e.g., S. W. Lovesey, *Theory of Neutron Scattering from Condensed Matter* (Clarendon, Oxford, 1984).

¹⁴G. L. McPherson and K. O. Devaney, *Inorg. Chem.* **16**, 1565 (1977).

¹⁵M. J. Hennessy, C. D. McElwee, and P. M. Richards, *Phys. Rev. B* **7**, 930 (1973).

¹⁶B. D. Gaulin and M. F. Collins, *Phys. Rev. B* **33**, 6287 (1986).

¹⁷N. Achiwa, *J. Phys. Soc. Jpn.* **27**, 561 (1969).

¹⁸R. E. Dietz, L. R. Walker, F. S. L. Hsu, W. H. Haemmerle, B. Vis, C. K. Chan, and H. Weinstock, *Solid State Commun.* **15**, 1185 (1974).

¹⁹U. Falk, A. Furrer, J. K. Kjems, and H. U. Güdel, *Phys. Rev. Lett.* **52**, 1336 (1984).